Charge transport through small silicon clusters

Christopher Roland,[1] Vincent Meunier,[1] Brian Larade,[2] and Hong Guo[2]
[1]*Department of Physics, The North Carolina State University, Raleigh, North Carolina 27695*
[2]*Center for the Physics of Materials and Department of Physics, McGill University, Montreal, PQ, Canada H3A 2T8*
(Received 18 December 2001; published 29 July 2002)

With a recently developed *ab initio* nonequilibrium Green's-function formalism, we have investigated the transport behavior of small Si_n, $n=1-10$, 13, and 20 nanoclusters between atomistic Al and Au leads. All of the clusters display metallic *I-V* characteristics, with typical conductances ranging between two and three (units of $G_o=2e^2/h$). The transport properties of these cluster junctions may be understood in terms of both the band structure of the electrodes, and the molecular electronic states of the clusters as modified by the lead environment. In addition, the quantum transport properties of Si nanoclusters doped with a Na atom are also analyzed.

DOI: 10.1103/PhysRevB.66.035332 PACS number(s): 73.61.Wp, 73.23.Ad, 72.80.Rj

I. INTRODUCTION

There is considerable interest in the geometrical, electronic, and chemical properties of nanoscale clusters. Such clusters represent an intermediate phase of matter, whose material properties are often quite different from either the single-atom or bulk properties of the elements involved.[1] With the current scientific focus on nanotechnology, the field of cluster research has received renewed impetus, as clusters may well provide suitable building blocks for the construction of desirable nanostructures. It is in this context that the quantum transport properties of nanoscale clusters may well prove to be important. The recent advent of molecular electronic systems has opened up a frontier in which atoms, clusters, and/or molecules assume the role of electronic device elements.[2–5] Progress in this field has been rapid, and already prototypical molecular logic circuits have been constructed in the laboratory. However, there remain many outstanding issues that need to be understood. In a nutshell, given a particular materials system, it is important to understand at a *microscopic* level—with as few adjustable parameters as possible—all the relevant aspects which contribute to the electron transport through the system. This involves an investigation not only of the role of the different electronic levels of the system, but also how these change when coupled to different electrode environments.

In this paper, we present an *ab initio* investigation of the transport properties of small Si_n nanoclusters, with $n=1-10$, 13, and 20, between Al and Au (100) electrodes. Because Si is a semiconducting material of great technological importance, Si clusters have been investigated quite extensively, both experimentally[6–11] and theoretically.[12–24] Indeed, the structure and properties of small Si_n clusters, with $n\leqslant 10$, are now well understood, so that recent investigations have focused on clusters of a more intermediate size with $n=20-30$,[24] larger clusters,[25,26] and on the more exotic Si cages.[27] Our results show that small Si nanoclusters act primarily as metals, with typical conductances ranging between 2 and 4 in units of $G_o=2e^2/h\approx(12.9\ \mathrm{k}\Omega)^{-1}$. For the case of Al and Au (100) electrodes, there appears to be little charge doping of the Si system, and the transmission spectrum may be understood both in terms of the bandstructure of the leads as well as the renormalized molecular levels[28] (RML's) of the Si clusters.

The following is a brief outline of the paper. After a brief discussion of the methodology, we discuss the transport through small Si_n clusters as well as through the more intermediate Si_{20} clusters (Sec. III). Section IV discusses quantum transport through Si clusters doped with a Na atom, while Sec. V is reserved for a short summary.

II. METHODOLOGY

Our investigations are based on a recently developed *ab initio* formalism,[29,30] which combines the Keldysh nonequilibrium Green's function theory (NEGF) (Refs. 32–34) with real-space density-functional-theory (DFT) simulation methods. As the details of this technique are somewhat technical and have been published elsewhere, we simply present a brief summary of the method, and otherwise refer the interested reader to Refs. 29 and 30.

The molecular device is divided into three regions: a left lead, a right lead, and a central scattering region. It is important to note that the central scattering region contains a portion of the semi-infinite leads, as shown in Fig. 1. Care must be taken so that this part of the scattering region is large enough so that effects of the cluster to the Kohn-Sham potential outside the scattering region is screened, and the po-

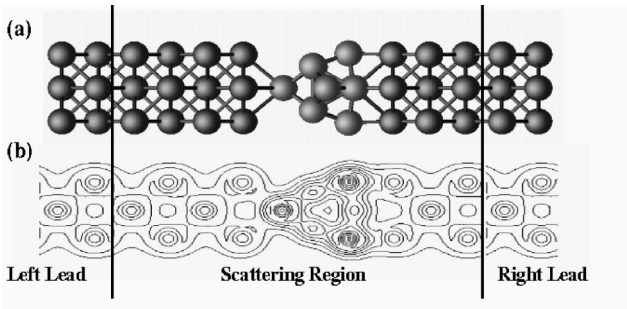

FIG. 1. (a) Schematic plot of the $Al(100)/Si_{10}$ molecular device. (b) Contour plot of a slice of the equilibrium charge distribution. Note the almost perfect match across the boundaries of the central scattering region and leads.

tential is well approximated by that of a perfect bulk electrode environment. The latter is determined via a separate calculation.[31] The scattering system is then converged via standard DFT methods to within 10^{-3} eV, thereby establishing the bonding between the molecules and the electrodes, the common Fermi level, and charge neutrality at equilibrium. The Kohn-Sham potential outside the scattering region is set to the bulk value, along with a proper matching of the electrostatic potential at the boundary. The *infinite* open boundary problem is thereby reduced to a proper, self-consistent calculation of the charge density for the *finite-sized* scattering region.

To calculate the charge density ρ it is convenient to use the NEGF formalism, which shows that

$$\rho = \frac{-i}{2\pi}\int dE\, G^{<}(E) = \frac{-i}{2\pi}\int dE\, \mathbf{G^R \Sigma^< G^A}$$

with $\mathbf{G^{R,A}}$ denoting the retarded/advanced Green's function of the device, and with $\Sigma^{<} = -2i\,\mathrm{Im}(f_l\Sigma^l + f_r\Sigma^r)$ the lesser self-energy of the system. Here $\Sigma^{l,r}$ represents the self-energies due to the couplings to the left and right electrodes, respectively, and $f_{l,r}$ the corresponding electron distribution describing the occupation of the eigenstates of each of the electrodes. It is important to note that this formalism allows for the computationally efficient evaluation of the contributions of not only the *scattering* states of the system, but also the *bound* states. The latter is accomplished via a direct numerical evaluation of a suitable contour integral.[30]

To calculate the needed quantities, a minimal *s*, *p*, and *d* Fireball basis set is used along with standard norm-conserving pseudopotentials for the atomic cores in order to expand the electronic wave functions and construct the Hamiltonian matrix. The Green's functions of the system may then be calculated by a direct matrix inversion, while the self-energies are calculated via standarded iterative technique. Once DFT self-consistancy is reached, the electric current is evaluated using the Landauer formula

$$I = \frac{2e}{h}\int_{\mu_{min}}^{\mu_{max}} dE(f_l - f_r)T(E,V_b)$$

where the transmission probability $T(E)$ as a function of electron energy E is given by

$$T(E,V_b) = 4\ \mathrm{Tr}[\mathrm{Im}(\Sigma_l G^R \Sigma_r G^A],$$

and $\mu_{min} = \min(\mu + V_b, \mu)$ and $\mu_{max} = \max(\mu + V_b, \mu)$ represents the minimum and maximum electrochemical potential of the leads. Here we have written μ as the chemical potential for each of the (same) leads, and applied the bias voltage V_b to the left lead. At equilibrium, the current is proportional to the conductance G, which is evaluated at the Fermi level of the device:

$$G(\mu) = \frac{2e^2}{h}T(\mu).$$

The method has previously been used to investigate quantum transport through fullerene cages,[28,29,35] linear C chains,[36] and Si nanowires.[37]

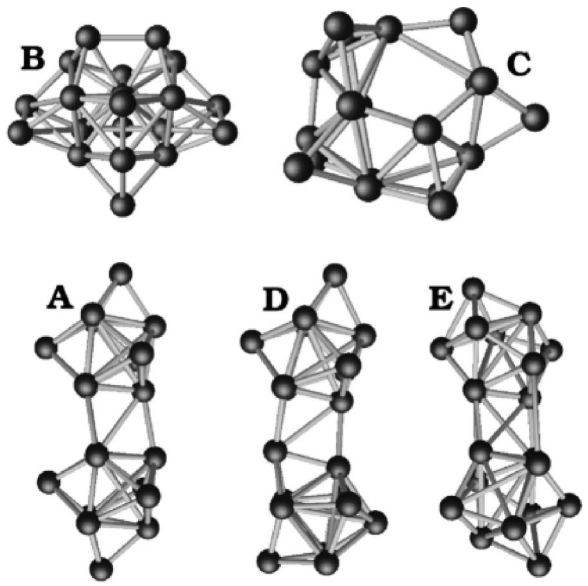

FIG. 2. Structures of the five low-energy isomers of the Si_{20} clusters considered.

III. TRANSPORT THROUGH Si_N CLUSTERS

To construct the two-probe devices, DFT-relaxed isolated Si_n clusters, with $n \leqslant 10,13,20$, were placed between two Al(100) leads, as shown in Fig. 1. Generally speaking, only the ground-state configurations were considered, and placed such that the Si atoms protruding from the cluster were a distance of 4.215 a.u. away from the center of each of the electrodes. For Si_{10} and Si_{13}, two different isomers were considered; for Si_{20}—which represent clusters of intermediate size—the five isomers shown in Fig. 2 were investigated. What is particularly interesting about the Si_{20} isomers is that these clusters represent a transition from a more *prolate* to a more *oblate* structure. Hence, isomers A, B, and C all represent elongated structures consisting of two compact Si_n clusters with $n \approx 10$ atoms brought together. Isomers B and C, by contrast, are similar to the smaller Si_n clusters in that they are much more compact. While DFT methods predict isomer B to be the ground-state structure, and Hartree-Fock calculations favor isomer C, highly accurate quantum Monte Carlo methods show that isomer E is in fact the ground-state cluster.[24] In addition, the transport properties of selected Si clusters in different orientations were also studied. This is particularly easy for Si_{2-4}. For instance, while the plane of these clusters is for the most part oriented perpendicular to the plane of the electrode atoms, we also examined configurations in which this plane is *parallel*. We will refer to results obtained with this orientation with a v, i.e., Si_3 (perpendicular) versus Si_3v (parallel). In addition, for Si_3, we considered a configuration for Si_3 in which the two Si atoms emanating from the vertex are oriented symmetrically with respect to the second electrode, and denote this configuration by Si_3s. Finally, we note that we also investigated transport through a select number of clusters placed between Au(100) leads.

When discussing transport through nanosystems, it is important to first consider the properties of the electrodes. In our case, the Al(100) leads simply act as metallic nanowires

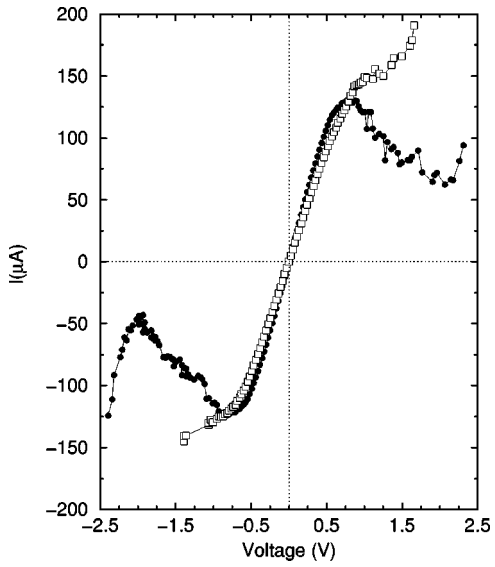

FIG. 3. Sample *I-V* curves for Si nanoclusters between Al(100) leads: filled circles, Si_4; squares, Si_7.

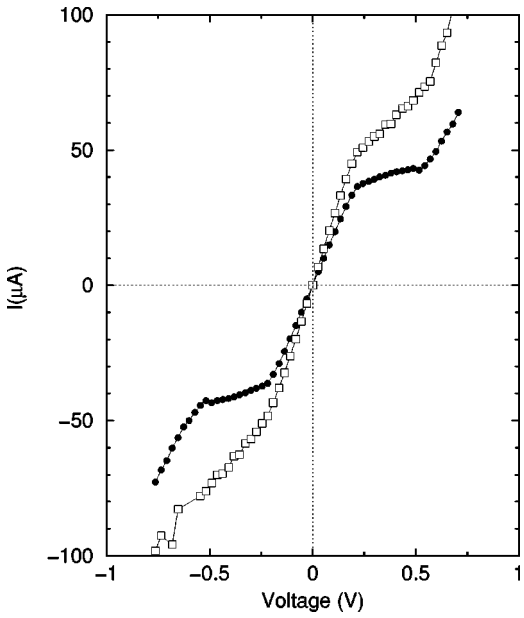

FIG. 4. Sample *I-V* curves for Si nanoclusters between Au(100) leads: filled circles, Si_4; squares, Si_7.

with linear current-voltage (*I-V*) characteristics and $G = 7G_o$, showing that when the electron energy is aligned with the Fermi level, transport takes place uniformly through all of the available energy bands.

All of the clusters investigated display qualitatively similar behavior, with typical *I-V* curves for two Si clusters ($n = 4$, and 7) shown in Fig. 3. The *I-V* curves all display a linear region centered about $V = 0$, and different types of *nonlinear* behavior out at the higher bias voltages. For the cases of Si_4, there is definite evidence for negative differential resistance (NDR) for bias voltages between ~ 0.8 and 2.1 V and ~ -0.8 and -2.0 V. For $V \geqslant 2.1$ and $V \leqslant -2.0$, there is a definite change and the current once again increases (decreases) with increasing (decreasing) voltage for positive (negative) voltages, respectively. In contrast, the Si_7 clusters shows no evidence of NDR. Instead, there is simply a marked decrease in the slope for *V* between ~ 0.82 and 1.56. For larger voltages, this slope appears to increase once again. Figure 4 shows similar results for Si_4 and Si_7, but now between Au(100) electrodes. The *I-V* curves are similar to those between the Al leads in that there is a central linear regime, with nonlinear behavior out on the wings. In this case there is no evidence of NDR, but simply variations in the slope.

The low-bias *I-V* characteristics for all the clusters is *linear*—which is characteristic of *metallic* behavior. Hence the transport properties for low bias voltages are best described by their conductances (G), which are summarized in Table I. For the most part, these fall between $2.0G_o$ and $3.5G_o$, showing that there are *less* channels open for transport through the clusters than through the straight Al nanowires we take for the leads. Most of the voltage drops in the system will therefore take place at the Al/Si interfaces.

Roughly speaking, clusters with similar structures display similar transport properties. For instance, Si_2 and Si_3 are the same, except that Si_3 has an additional Si atom pointing off to the side. The effect of this is to reduce G somewhat by a relatively small factor of $0.25G_o$. By rotating the Si_3 cluster slightly in order to bring two (instead of one) Si atoms within the interaction range forming Si_3s, the conductance increases and becomes comparable to that of Si_2. Similarly, rotating the clusters so that they are positioned in a plane parallel to the Al(100) surface, as in the $Si_{2\text{-}4}v$ structures, always leads to an increase in the conduction as more atoms are brought into the interaction range. By the same token, one may think of the $Si_{4\text{-}7}$ clusters as building upon the planar D_{2h} structure of Si_4. Hence all of these clusters display relatively similar conductances. The largest differences in properties are dis-

TABLE I. *Ab initio* conductances G of small Si_n clusters of a given symmetry (Sym) between Al (100) electrodes in units of G_o.

Si_n	Si_1	Si_2	Si_2v	Si_3	Si_3s
Sym.				C_{2v}	C_{2v}
G	2.04	2.52	2.66	2.25	2.63
Si_n	Si_3v	Si_4	Si_4v	Si_5	Si_6
Sym.	C_{2v}	D_{2h}	D_{2h}	D_{3h}	C_{2v}
G	2.92	2.77	2.92	2.88	3.01
Si_n	Si_7	Si_8	Si_9	Si_{10}	Si_{10}
Sym.	D_{5h}	C_{2h}	C_{2v}	C_{3v}	T_d
G	2.82	1.95	2.81	2.22	3.14
Si_n	Si_{13}	Si_{13}	Si_{20}	Si_{20}	Si_{20}
Sym.	C_{3v}	I_{2h}	A	B	C
G	1.43	3.15	2.18	1.79	1.21
Si_n	Si_{20}	Si_{20}			
Sym.	D	E			
G	1.85	0.31			

TABLE II. *Ab initio* conductances G (units G_o) of a Si_6 cluster as a function of the cluster-electrode distance d (a.u.). Here $\Delta Q-i$ indicates the charge difference on the ith Si atom in the cluster. The structure of Si_6 is shown in Fig. 1(a); atoms 1 and 2 are closest to the electrodes; and atoms 3 and 4 and 5 and 6 are opposite each other.

d (a.u.)	2.215	3.215	4.215	5.215	6.215
G	3.36	2.71	3.01	0.95	0.11
$\Delta Q-1$	0.647	0.331	0.128	0.016	-0.035
-2	0.647	0.331	0.128	0.018	-0.033
-3	0.045	0.056	0.103	0.141	0.156
-4	0.045	0.056	0.103	0.141	0.156
-5	-0.100	-0.105	-0.089	-0.072	-0.072
-6	-0.099	-0.105	-0.088	-0.072	-0.072

played by the two isomers of the Si_{10} and Si_{13} clusters. The difference in this case is accounted for by the relative compactness of $Si_{10}T_d$ and $Si_{13}I_{2h}$ clusters. For these isomers, there are at least three Si atoms within interaction range at each of Si/Al interfaces, while the $Si_{10,13}C_{3v}$ clusters have at least one interface with only one to two atoms within a similar range. This decrease in the number of atoms close to the Al interface accounts for the corresponding decrease in G for these clusters.

In contrast to C-based systems such as linear chains of C atoms[36,38] and/or fullerenes,[29,35] there appears to be little charge transfer between the Si_n clusters and the Al electrodes. For all the clusters, the Fermi level is below that of the Al electrodes. There is however, only a small amount of charge—between 0.1 and 0.2 electrons—transferred to the Si atoms closest to the electrodes. These observations on the charge transfer are consistent with a recent study of transport through H-terminated Si nanowires,[39] also coupled to Al leads. The amount of charge transfered varies only slightly with respect to the applied voltage. It does, however, depend somewhat on the cluster-electrode distance (d), as summarized in Table II. Here we see that G is maximized near a $d \approx 4.215$ a.u., and decreases rapidly as d is increased. G does, however, increase slightly as d is decreased. Also note that the charge transfered to the Si atoms 1 and 2—which are the atoms closest to the electrodes as shown in Fig. 1(a)—also increases as d is decreased. However, in this case this only leads to a relatively modest increase in G. Comparable results are obtained for the other Si_n clusters. These results are to be contrasted with the fullerene systems such as the C_{20} chains,[35] which are highly electronegative and soak up to about three electrons from the same leads, which makes those I-V characteristics very sensitive to the parameter d. By contrast, the transport properties of the Si clusters are a lot less sensitive to this parameter, because charge doping definately plays a much more secondary role.

How can we explain the shape of the I-V curves? In order to understand these, we have analyzed the transmission coefficients $T(E,V_b)$, which gives contributions to the current as a function of the electron energy and bias voltage. Generally speaking, this function shows considerable variations as a function of E, but relatively little as a function of V_b—at least for small bias voltages. Hence we have concentrated on understanding $T(E)$ at constant V_b. We find that these curves may be understood in terms of two simple concepts, namely the *band structure* of the leads and the *renormalized molecular levels*[28] which mediate the transmission process.

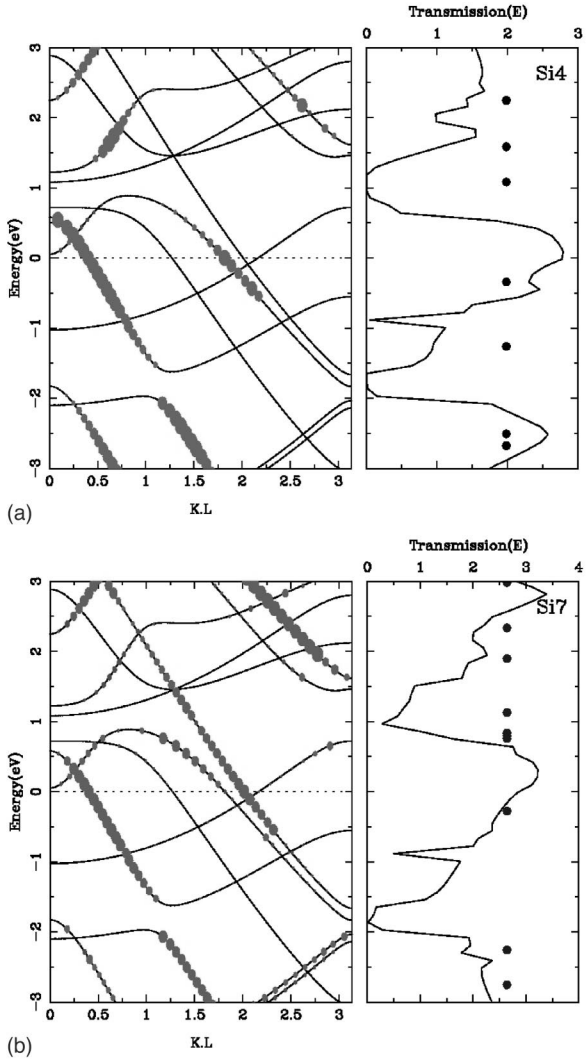

FIG. 5. Band structure of Al(100) electrodes (left panel) along with the corresponding transmission function $T(E)$ (right panel). On the band structure the wave vectors corresponding to the scattering states are marked with a filled circles, with the size indicating the relative importance of the state for the transmission process. On the right panel, the RML's are marked with filled circles. We show plots for clusters: (a) Si_4 and (b) Si_7s.

Figure 5 shows $T(E)$ (right panel) for Si_4 and Si_7, along with the band structure (left panel) of the Al(100) leads for wave vectors in the device direction. On the band structure, we have marked the wave vectors that couple to the scattering states of the system with filled circles such that the size of these circles indicates the relative importance of the state to the transmission process. What do we observe? For Si_4, there are *two* bands that significantly contribute to the transmission near the Fermi level, which is shifted to $E=0$. The contributions from the other bands is considerably less, and

hence $T(E)$ may be expected to take on a value greater than $2G_o$, which is what is observed. Similarly, for Si_7, many more bands contribute to the transmission giving a larger value of $\sim 3.5G_o$. The linearly increasing parts of the I-V curve may now be readily understood. As the bias voltage increases, the relative position of the bandstructure of the left- and right-electrodes are shifted apart by the bias. Between $E=0$ and ~ 0.46 eV, the current increases because more and more conduction band density of states are included in the integration window. However, for $V \sim 0.46$ eV, there are no additional conduction density of states, because no scattering states in that region couple to the molecule. Clearly $T(E)$ must decrease precipitiously at that point, and the current begins to drop. The system then displays a significant NDR until $E \sim 2$ eV, when the current once again begins to recover. Contrast this behavior with the results for the Si_7 cluster device. For small bias voltages, the system is characterized by a linear region, similar to that of the Si_4 cluster. However, for $E \geqslant 0.5$ eV, there is always at least one band that conducts significantly. Hence, although $T(E)$ does decrease significantly, it does not go to zero as in the previous case. This decrease in T here manifests itself through a decrease in the *slope* of the I-V curves, and not a NDR. After $E \geqslant 1.5$ eV, once again many more bands contribute to the transmission process, which is signaled through a further increase in the slope. Similar analysis explains the shape of the I-V curves for Si_4 and Si_7 clusters between Au leads, as shown in Figs. 4 and 6. Similar to the case of Si_7 clusters between Al leads, the I-V curves display three region: a linear region about $V=0$, a region with reduced slope, and a third region in which the slope increases once again. As shown in Fig. 6, the shape of these curves may also be understood in terms of the band structure of the Au leads, which of course is completely different from the case of the Al electrodes. These considerations clearly emphasize the fact that a fully atomistic description of the leads is important in order to truly understand the transport characteristics of molecular electronic systems.

The second aspect important for understanding the I-V curves are the molecular levels important for the transmission process. To understand this point, consider an isolated molecular cluster. For such a system, it is relatively easy to find the molecular levels by simply diagonalizing the Hamiltonian of the system and thereby identifying the highest occupied molecular orbital (HOMO) and lowest unoccupied molecular orbital (LUMO). These levels may not, however, be exactly the levels relevant for the transmission process. Because of the coupling between the electrodes and the molecule, the character of these levels will change considerably in ways that are not known *a priori*. Furthermore, the energy spectrum for the open quantum system will be continuous, and broadened because of the contact to the leads. In order to understand these changes, we have concentrated on finding the renormalized molecular levels[28] which are calculated as follows. After the self-consistent cycle of the Kohn-Sham equations is completed, one obtains the self-consistent effective potential along with the matrix elements of the Hamiltonian. By diagonalizing the submatrix of the Hamiltonian associated with the atomic orbitals of the Si cluster, one obtains a set of levels—the renormalized molecular levels—which are indicative of the changes induced in the molecular levels of the isolated cluster by the coupling to electrode system.

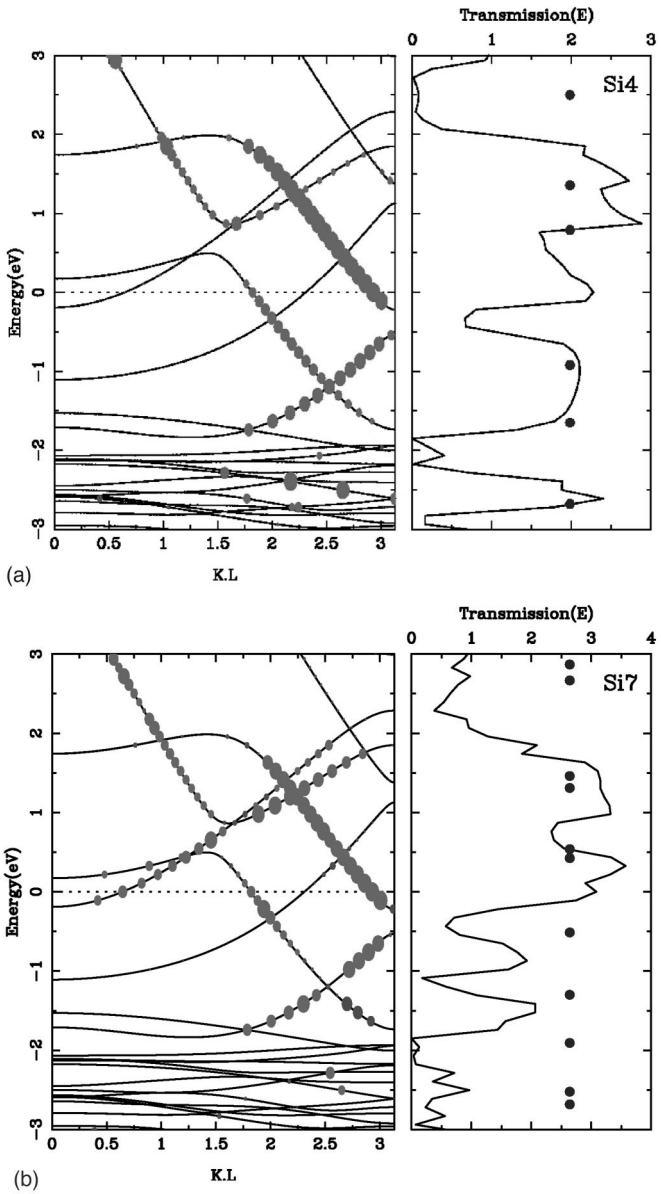

FIG. 6. Same as Fig. 5, except that results are for systems with Au(100) leads: (a) Si_4. (b) Si_7.

It is evident from Figs. 5 and 6 that many of the peaks observed of $T(E)$ correspond (roughly) to a location of a RML for the given Si cluster. Hence, the position of a RML typically marks a broad region in energy over which there is significant coupling betwen the electronic states of the clusters and the leads. As the clusters become larger, the number of RML's begins to proliferate, and many individual peaks associated with the RML's become discernable. Of course, the position of the RML's is sensitive to the orientation of the cluster. We also note that the presence of an RML is a necessary, but not sufficient condition for a transmission peak, i.e., not all RML's contribute to the conduction process.

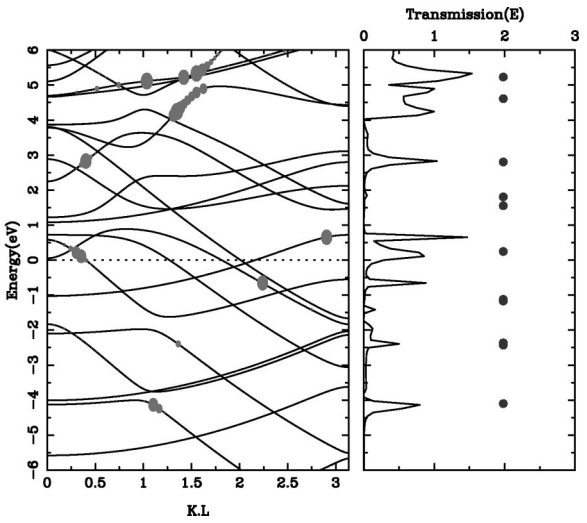

FIG. 7. Band structure and $T(E)$ for a Si_4 cluster, but with an increased Al(100)/Si_4 distance. This $T(E)$ should be compared to that shown in Fig. 5, and the change in peak structure and position noted.

It is of interest to understand the origins of the RML's that are most important for transmission. We have therefore examined the relation of the RML's to the original molecular levels of the isolated molecule.[28] Generally speaking, the six states closest to the HOMO/LUMO gap of the original molecular levels of the isolated Si clusters provide the major contribution to the different RML's. However, there does not appear to be a clear pattern concerning the nature of these RML's with respect to the size of the different clusters, although for the most part these correspond to a given molecular level that has been shifted upwards in energy by a fraction of an eV. The influence of the lead in forming the different RML's can also be probed by changing the electrode/cluster distance. When this distance is increased, the influence of the leads on the RML's should lessen. And that is indeed what we observe. As this distance is increased, the number of scattering states that couple to each of the RML's is reduced, so that $T(E)$ is characterized by a set of resonant peaks that appear to interpolate smoothly on the molecular levels of the isolated cluster. An example of this is shown in Fig. 7.

IV. NA-DOPED Si_N CLUSTERS

A common strategy for changing the transport properties of materials is to add impurity atoms to the system, which either donate or remove charges, thereby altering the molecular levels through which electrons flow. As a paradigmatic example of such a system, we considered the transport through Si_n clusters doped with a single Na atom. Because Na is highly electropositive, it is expected to readily give up its valence electron. The appropriate clusters were formed by fully relaxing the Si_nNa structures within density-functional theory, which yielded configurations similar to those reported in the literature.[39] For the most part, the transport characteristics of the Si_nNa clusters share many common features with those of the undoped system, showing that a single Na atom does not perturb the clusters significantly. Hence the *I-V* characteristics for small bias voltages are again linear with corresponding *G*'s for selected clusters given in Table III. For the most part, the *G*'s are slightly reduced when compared to the corresponding clusters without the Na atom. In terms of charge transfer, the Na atom does indeed lose most of its valence electron to its surroundings. This is particularly for cases when the Na is close to the Al(100) electrodes, when practically all of its electron is lost. However, as the number of Si atoms in the cluster increases, the charge transfer from the Na is somewhat reduced with typical values corresponding to $\sim 0.8e-0.6e$. For the most part, the charge distribution for the Si atoms is similar to that of the undoped systems, with an overall increase of $\sim 0.1e$ over the undoped case for the Si atoms closest to the electrodes. The transfer of charge from the electrodes, however, seems to be reduced. The doping of Si clusters with a single Na atom Si clusters with a single Na atom does not appear effective in modifying the transport properties of the clusters.

TABLE III. *Ab initio* conductances *G* (units G_o) of selected Si_n clusters between Al(100) electrodes doped with a single Na atom. Here $(Si_1Na)v$ and $(Si_1Na)h$ are similar to configurations Si_2v and Si_2 as explained in the text, but with a Na atom replacing one of the Si atoms. Note the almost order of magnitude difference in *G* between the two configurations. Also, the orientation for the (Si_8Na) clusters is not directly comparable to that of Si_8 in Table I. Because of differences in orientation, there are more Si atoms closer to the electrodes for the Si_8Na, case accounting for the very large increase in *G*.

Si_nNa	Si_1v	Si_1h	Si_2	Si_3	Si_5
G	3.39	0.32	2.46	1.90	1.84
Si_nNa	Si_6	Si_8	$Si_{10}C_{2v}$		
G	2.72	3.31	2.50		

V. SUMMARY

In summary, we have examined the transport properties of small Si_n, $n \leqslant 10,13,20$ clusters between Al(100) leads. The *I-V* curves for all of these clusters is linear—characteristic of metallic systems—about $V=0$. Nonlinear behavior, including NDR, is observed for large bias voltages. The slopes, i.e., the conductances for small bias voltages are all between 2 and 4 in units of G_o. In contrast to C-based systems, there appears to be little charge doping betwen the leads and the clusters. The shape of the *I-V* curves may be understood in terms of the band structure of the leads, and the RML's of the open quantum system. Finally, we have also examined transport through Si_nNa clusters, in which the Na atom readily gives up its valence electron to the system. This, however, does not lead to significant changes in the transport properties of the Si clusters.

ACKNOWLEDGMENTS

We thank both C.Z. Wang and L. Mitas for providing us with the coordinates for relaxed Si clusters. We acknowledge financial support from the U.S. DOE and NSF (C.R.), and NSERC of Canada and FCAR of Quebec (H.G.). We also thank the North Carolina Supercomputing Center (NCSC) for extensive computer time.

[1] M.F. Jarrold, Science **252**, 1085 (1991); J. Phys. Chem. **23**, 918 (1991).
[2] C.P. Collier, G. Mattersteig, E.W. Wong, Y. Luo, K. Beverly, J. Sampaio, F.M. Raymo, J.F. Stoddart, and J.R. Heath, Science **289**, 1172 (2000).
[3] M.A. Reed, C. Zhou, and J. Muller, Science **278**, 252 (1997); J. Chen, M.A. Reed, and A.M. Rawlett, Science **286**, 1550 (1999).
[4] C. Joachim, J.K. Gimzewski, R.R. Chlitter, and C. Chavy, Phys. Rev. Lett. **74**, 2102 (1995); J.K. Gimzewski and C. Joachim, Science **283**, 1683 (1999).
[5] T. Ruekes, K. Kim, E. Joselvich, G.Y. Tseng, C.-L. Cheung, and C.M. Lieber, Science **289**, 94 (2000).
[6] M.F. Jarrold, J. Phys. Chem. **99**, 11 (1995).
[7] K.M. Ho, A.A. Shvartsburg, B. Pan, Z.Y. Lu, C.Z. Wang, J.G. Wacker, J.L. Fye, and M.F. Jarrold, Nature (London) **392**, 582 (1998).
[8] A.A. Shvartsburg, M.F. Jarrold, B. Liu, Z.Y. Lu, C.Z. Wang, and K.M. Ho, Phys. Rev. Lett. **81**, 4616 (1998).
[9] E.C. Honea, A. Ocura, C.A. Murray, K. Raghavachari, W.O. Sprenger, M.F. Jarrold, and W.L. Brown, Nature (London) **366**, 42 (1993).
[10] O. Cheshnovsky, S.H. Yang, C.L. Pettiette, M.J. Craycraft, Y. Liu, and R.E. Smalley, Chem. Phys. Lett. **138**, 119 (1987).
[11] L.P. Rokhinson, L.J. Guo, S.Y. Chou, and D.C. Tsui, Phys. Rev. B **63**, 035321 (2001).
[12] J.C. Phillips, J. Chem. Phys. **87**, 1712 (1987); J.R. Chelikowsky and J.C. Phillips, Phys. Rev. Lett. **63**, 1653 (1989).
[13] K. Ragavachari and V. Logovinsky, Phys. Rev. Lett. **55**, 2853 (1985); K. Raghavachari, J. Chem. Phys. **84**, 5672 (1986); K. Raghavachari and C.M. Rohlfing, *ibid.* **89**, 2219 (1988); L.A. Curtiss, P.W. Deutsch, and K. Raghavachari, *ibid.* **96**, 6868 (1992).
[14] D. Tomanek and M. Schluter, Phys. Rev. Lett. **56**, 1055 (1986); Phys. Rev. B **36**, 1208 (1987); Phys. Rev. Lett. **67**, 2331 (1991).
[15] P. Ballone, W. Andreoni, R. Car, and M. Parrinello, Phys. Rev. Lett. **60**, 271 (1988); W. Andreoni and G. Pastore, Phys. Rev. B **41**, 10 243 (1990).
[16] U. Rothlisberger, W. Andreoni, and P. Giannozzi, J. Chem. Phys. **96**, 1248 (1992).
[17] N. Binggeli, J.L. Martins, and J.R. Chelikowsky, Phys. Rev. Lett. **68**, 2956 (1992); N. Binggeli and J.R. Chelikowsky, Phys. Rev. B **50**, 11 764 (1994).
[18] E. Kaxiras and K. Jackson, Phys. Rev. Lett. **71**, 727 (1993).
[19] N. Govind, J.-L. Mozos, and H. Guo, Phys. Rev. B **51**, 7101 (1995).
[20] M. Menon and K.R. Subbaswamy, Phys. Rev. B **47**, 12 754 (1993); P. Ordejon, D. Lebedenko, and M. Menon, *ibid.* **50**, 5645 (1994).
[21] M.V. Ramakrishna and J. Pan, J. Chem. Phys. **101**, 8108 (1994).
[22] S. Wei, R.N. Barnett, and U. Landman, Phys. Rev. B **55**, 7935 (1997).
[23] Z.-Y. Lu, C.Z. Wang, and K.-M. Ho, Phys. Rev. B **61**, 2329 (2000).
[24] L. Mitas, J.C. Grossman, I. Stich, and J. Tobik, Phys. Rev. Lett. **84**, 1479 (2000).
[25] U. Rothlisberger, W. Andreoni, and M. Parrinello, Phys. Rev. Lett. **72**, 665 (1994).
[26] E. Kaxiras, Phys. Rev. B **56**, 13 455 (1997).
[27] H. Hiura, T. Miyazaki, and T. Kanayama, Phys. Rev. Lett. **86**, 1733 (2001).
[28] B. Larade, J. Taylor, Q.R. Zheng, H. Mehrez, P. Pomorski, and H. Guo, Phys. Rev. B **64**, 195402 (2001).
[29] J. Taylor, H. Guo, and J. Wang, Phys. Rev. B **63**, 121104 (2001).
[30] J. Taylor, H. Guo, and J. Wang, Phys. Rev. B **63**, 245407 (2001).
[31] A.P. Jauho, N.S. Wingreen, and Y. Meir, Phys. Rev. B **50**, 5528 (1994).
[32] S. Datta, *Electronic Transport in Mesoscopic Systems* (Cambridge University Press, New York, 1995).
[33] B.G. Wang, J. Wang, and H. Guo, Phys. Rev. Lett. **82**, 398 (1999); J. Appl. Phys. **86**, 5094 (1999).
[34] In order to ensure good matching between the leads and scattering region, care must be taken that leads are described with a sufficiently high number of k points. We have used at least 500 points for the calculations presented here.
[35] C. Roland, B. Larade, J. Taylor, and H. Guo, Phys. Rev. B **65**, 041401 (2002).
[36] B. Larade, J. Taylor, H. Mehrez, and H. Guo, Phys. Rev. B **64**, 075420 (2001).
[37] P. Pomorski, B. Larade, J. Taylor, and H. Guo (unpublished).
[38] N.D. Lang and Ph. Avouris, Phys. Rev. Lett. **81**, 3515 (1998); **84**, 358 (2000).
[39] U. Landman, R.N. Barnett, A.G. Scherbakov, and Ph. Avouris, Phys. Rev. Lett. **85**, 1958 (2000).